

Band Gap of β -PtO₂ from First-principles

Yong Yang¹, Osamu Sugino^{1,2}, and Takahisa Ohno^{1,3}

¹*Global Research Center for Environment and Energy based on Nanomaterials Science (GREEN), National Institute for Materials Science (NIMS), Tsukuba, 305-0047, Japan*

²*Institute for Solid State Physics, University of Tokyo, 5-1-5 Kashiwanoha, Kashiwa 277-8581, Japan*

³*Computational Materials Science Unit, National Institute for Materials Science (NIMS), Tsukuba, 305-0047, Japan*

We studied the band gap of β -PtO₂ using first-principles calculations based on density functional theory (DFT). The results are obtained within the framework of generalized gradient approximation (GGA), GGA+U, *GW* and the hybrid functional method. For different types of calculations, the calculated band gap increases from ~ 0.46 eV to 1.80 eV. In particular, the band gap by *GW* (conventional and self-consistent) calculation shows a tendency of converging to $\sim 1.25 \pm 0.05$ eV. Effect of the on-site Coulomb interaction on the bonding characteristics is also analyzed.

PACS numbers: 61.66.Fn, 71.15.Qe, 71.15.Mb

In recent years platinum dioxides have attracted considerable attention as a catalytic material for chemical reactions on surface/interface [1-8]. Actually, PtO_2 is known as Adam's Catalyst [9, 10] in organic synthesis for a long time. For the oxidation of molecules on oxide surface, experiments have shown that the existence of PtO_2 can enhance the catalytic oxidation of carbon monoxide (CO) molecules [1], whose mechanism was theoretically explained later [2, 3]. In contrast to CO, the oxidation of NO molecules on PtO_2 (110) was theoretically predicted to be in a lower activity with comparison to that on pure Pt(111) surface [5]. The thin film of platinum oxide is observed to widely present on platinum electrode during electrochemical process [11], especially in the application of fuel cell [7, 8], which is an environmental friendly power resource. However, the effect of PtO_2 on the electrochemical processes, such as the oxygen reduction reaction (ORR) on Pt electrode, is poorly understood. As a first step, one should learn about the electronic properties of the material itself, which are, however, not yet well studied.

Experimentally, there are two crystalline phases of PtO_2 [12]: α - PtO_2 and β - PtO_2 . The crystal of β - PtO_2 adopts the orthorhombic CaCl_2 -type structure, which is distinguished from the other group VIII metal dioxides that have a tetragonal rutile structure [13]. Using density functional theory (DFT) calculations within the local density approximation (LDA), Wu and Weber explained the stability of the β - PtO_2 structure as originating from the strong hybridization between the Pt 5d and O 2p states around the Fermi level [14]. However, their calculated electronic density of states (DOS) indicates a metallic character of β - PtO_2 , which contradicts with the experimental measurement that β - PtO_2 is a semiconductor with a resistivity of $\sim 10^6 \Omega \cdot \text{cm}$ [15]. Until now, no experimental data is available for the band

gap of β -PtO₂, while the reported band gap of α -PtO₂ varies from ~ 1.3 eV [16] to 1.8 eV [17]. Our recent DFT-GGA calculation [18] with the PBE-type functional [19] gives a value of ~ 0.46 eV for β -PtO₂ band gap, which is further increased to be ~ 1.2 eV by using GGA+U scheme. The value of parameter U employed in the GGA+U calculation is justified [18] by using the conventional GW (G_0W_0) method [20, 21].

In this work, we go on to present a more comprehensive study on the band gap of β -PtO₂. In addition to GGA, GGA+U, and G_0W_0 , we have performed the self-consistent GW and the Heyd-Scuseria-Ernzerhof (HSE) type hybrid functional [22-24] calculations to make a comparison of the results of different methods. The calculations are carried out by the Vienna *ab initio* simulation package (VASP) [25, 26], using a plane wave basis set and the projector augmented-wave (PAW) potentials [27, 28]. The exchange-correlation interactions of valence electrons are described by the PBE-type functional [19] for the GGA calculations, and by the HSE03 [22, 23] and HSE06 [24] functionals for the hybrid functional calculations. While doing the GGA+U calculations, the on-site Coulomb repulsion is treated using the simplified scheme introduced by Dudarev *et al.* [29]. As for the GW calculations, we take both the conventional and the self-consistent GW approach implemented in VASP [30, 31] to calculate the energy spectrum of quasiparticle. The quasiparticle energies and wave functions are obtained by solving the following equation [21]:

$$(T + V_{ext} + V_H)\psi_{nk}(\vec{r}) + \int d\vec{r}' \Sigma(\vec{r}, \vec{r}'; E_{nk})\psi_{nk}(\vec{r}') = E_{nk}\psi_{nk}(\vec{r}),$$

where T is the kinetic energy operator of electrons, V_{ext} is the external potential due to ions, V_H is the electrostatic Hartree potential, Σ is the electron self-energy operator, and E_{nk} and $\psi_{nk}(\vec{r})$ are the quasiparticle energies and wave functions, respectively. Within the GW approximation, the self-energy operator Σ is expressed as follows:

$$\Sigma(\vec{r}, \vec{r}'; E) = \frac{i}{2\pi} \int d\omega e^{i\delta\omega} G(\vec{r}, \vec{r}'; E + \omega) W(\vec{r}, \vec{r}'; \omega),$$

where G is the Green's function, W is the screened Coulomb interaction, and δ is a positive infinitesimal. For the convenience of discussion, we take the commonly used symbol " G_0W_0 " for denoting the conventional GW , and " GW_0 " for the partially self-consistent GW , where the self-consistent iteration is done for G only, and " GW " for the fully self-consistent GW approach, where the self-consistent iteration is done for both G and W .

All the calculations are done for the primitive cell of β -PtO₂, which contains 2 Pt atoms and 4 O atoms. In both GGA and GGA+U calculations, we use a $16 \times 16 \times 16$ k-mesh and an energy cutoff of 600 eV for plane waves. In the HSE-type hybrid functional calculations, a $8 \times 8 \times 8$ k-mesh and an energy cutoff of 600 eV for plane waves are employed. In the GW calculations, because of the heavy computational burden, the employed k-meshes range from $2 \times 2 \times 2$ to $6 \times 6 \times 6$, and the energy cutoff for plane waves range from 300 eV to 800 eV, to test the convergence of obtained band gap. The k-meshes are generated by the Monkhorst-Pack scheme [32]. The tetrahedron method with Blöchl corrections [33] is used for doing integral in the Brillouin zone (BZ).

The primitive cell of β -PtO₂ is shown Fig. 1(a), in which every Pt atom is coordinated by six O atoms, and accordingly every O atom is coordinated by three Pt atoms. The

calculated band gap, and the optimized length of the orthorhombic cell edges a , b , and c with the GGA+U method are shown in Fig. 1(b) and Fig. 1(c), respectively, as a function of the effective on-site Coulomb repulsion (U_{eff}). The data points at which $U_{\text{eff}} = 0$ correspond to the pure DFT-GGA calculations. The band gap shows a general tendency of increasing with enlarged U_{eff} , and the calculated cell parameters a and c show a trend of decreasing with enlarged U_{eff} while the length of cell edge b fluctuates with U_{eff} . At the point where $U_{\text{eff}} = 7$ eV, there is a slight dip in the value of band gap. This is related to the structural relaxation of atoms and cell geometries. As shown in Fig. 1(c), the length of cell edge c increases slightly at $U_{\text{eff}} = 7$ eV with comparison to the value of c at $U_{\text{eff}} = 6.5$ eV, which is out of the general variation trend of dropping. When the atomic positions and cell parameters are kept the same for the calculations with different U_{eff} , we find that the dipping point vanishes and the band gap increases monotonically with increasing U_{eff} . The relaxed cell parameters by GGA+U calculations with the value of U_{eff} of about 7.5 eV match the experimental values best. In the following paragraphs, we will show that the calculated band gap with $U_{\text{eff}} = 7.5$ eV also agrees quite well with GW calculations.

Figure 2(a) shows the calculated electronic density of states (DOS) of β -PtO₂ using the conventional and self-consistent GW method (G_0W_0 , GW_0 , GW). Compared to the GGA band gap (0.46 eV) and the GGA+U band gap (1.20 eV) in our recent work [18], the calculated band gap by G_0W_0 , GW_0 , and GW is 1.31 eV, 1.45 eV, and 1.50 eV, respectively. A $4 \times 4 \times 4$ k-mesh and an energy cut-off of 600 eV for plane waves and totally 400 energy bands are used for the G_0W_0 , GW_0 , and GW calculations to obtain the data in Fig. 2(a). Calculated GGA energy bands along some symmetry lines in the BZ are shown in Fig. 2(b),

together with some G_0W_0 quasiparticle energy points. It is found that the energy dispersion of GGA and the G_0W_0 energy points is similar. Due to the usage of a smaller k-mesh, the GGA band gap deduced from Fig. 2(b) is ~ 0.7 eV, which indicates that the k-points corresponding to the band gap of ~ 0.46 eV in the more accurate DOS calculation are missing from the high symmetry lines. The key difference between GGA and G_0W_0 is that the G_0W_0 energies of the conduction bands are sitting at higher values. The partial DOS (PDOS) of Pt 5d and O 2p orbitals from GGA and GGA+U calculations are displayed in Figs. 2(c) and 2(d), respectively. Around the Fermi level, strong hybridization is found between the Pt 5d and O 2p orbitals in the GGA calculations. The Pt 5d and O 2p components in the bonding states near the Fermi level are almost the same for GGA. This implies that electron transfer can take place between the Pt 5d and O 2p orbitals with equal probability and magnitude. It is possible that the strong *pd* hybridization originates from the general trend that LDA/GGA insufficiently describes the interactions between the *d* electrons. Indeed, the GGA+U calculation provides qualitatively different DOS where the center of the Pt 5d bands is shifted downward by ~ 4 eV. This is presumably due to the Coulomb interaction of *d* electrons. As a result, the *pd* hybridization that appears in GGA is largely reduced, and the O 2p orbitals contribute to the major part of the electron DOS at energies ~ 2 to 3 eV below the Fermi level (Fig. 2(d)). Note that in ZnS [34] and ZnO [35] the *d*-bands were reported to be similarly shifted downward when the Coulomb interaction was incorporated by using the GGA+U method.

Figure 3 shows the DOS of β -PtO₂ calculated by using the HSE03 and HSE06 hybrid functionals. Below the Fermi level, the DOS from HSE03 and HSE06-type calculations are

almost the same. The features of the DOS above the Fermi level are also similar except that the bottom of conduction bands differs by ~ 0.2 eV. The calculated band gap is ~ 1.60 eV by HSE03 and is ~ 1.81 eV by HSE06. This indicates that, the HSE band gap depends notably on the empirical parameter μ [36] that defines the short-range and long-range Coulomb interactions in the exchange-correlation functional. The characteristic distance separating the short and long-range Coulomb interactions is $L_c = 2/\mu$, where $\mu = 0.3 \text{ \AA}^{-1}$ for HSE03 and $\mu = 0.2 \text{ \AA}^{-1}$ for HSE06. It follows that, $L_c \approx 6.67 \text{ \AA}$ for HSE03 and $L_c = 10 \text{ \AA}$ for HSE06.

To test the convergence of the computed G_0W_0 band gap, we have done calculations with varying energy cut-off of plane waves and k-meshes. Shown in Fig. 4(a), is the calculated electronic DOS diagrams at different energy cut-off using a $4 \times 4 \times 4$ k-mesh and 400 energy bands for the summation of quasiparticle energies. When the energy cut-off increases from 300 eV to 800 eV, the band gap is kept at ~ 1.3 eV, and the DOS features near the Fermi level is only slightly modified. That means, the energy cut-off of ~ 300 eV is enough for the G_0W_0 calculation of band gap. The variation of DOS with different k-meshes is shown in Fig. 4(b). The band gap varies from ~ 1.30 eV ($4 \times 4 \times 4$ k-mesh), and ~ 1.25 eV ($5 \times 5 \times 5$ k-mesh, run1 & run2), to ~ 1.22 eV ($6 \times 6 \times 6$ k-mesh). Calculation with finer k-meshes is not able to carry out, due to the quota of available computational resource. In spite of this limitation, the calculated G_0W_0 band gap shows a tendency of converging to ~ 1.2 eV. The partially self-consistent GW_0 gives a band gap of ~ 1.42 eV and 1.28 eV, for calculations using a $4 \times 4 \times 6$ and $6 \times 6 \times 6$ k-mesh, respectively. For a wide range of materials, the GW_0 usually give the best value of band gap comparing to experiment [31]. The self-

consistent GW band gap is ~ 1.46 eV by calculation using a $4\times 4\times 6$ k-mesh. Since the GW_0 and GW band gap is close to each other in calculations with the same k-mesh, we expect that the self-consistent GW band gap will converge to ~ 1.30 eV when calculated using a $6\times 6\times 6$ or denser k-meshes. In the following paragraphs, we will go on study the convergence of the G_0W_0 , which is computationally less demanding than the partially self-consistent GW_0 and the self-consistent GW method.

The convergent behavior of G_0W_0 calculation with respect to the number of bands can be very different from one system to another [30]. Recent studies on ZnO [35, 37] have shown that, the G_0W_0 band gap does not converge until a vastly large number of energy bands are included in the calculation. We have also made calculations to verify this point. Figure 5 shows the G_0W_0 band gap as a function of k-meshes and the number of energy bands employed in the calculation. For the $2\times 2\times 2$ and $3\times 3\times 3$ k-meshes, the calculated band gap fluctuates around 1.61 eV and 1.47 eV when the number of bands (NBAND) increases from 200 to 800. The band gap of $4\times 4\times 4$ k-mesh decreases continuously with increasing number of bands, from ~ 1.33 eV (NBAND = 200) to 1.27 eV (NBAND = 800). In the case of both $5\times 5\times 5$ and $6\times 6\times 6$ k-mesh, the parameter NBAND varies from 216 to 720. The calculated band gap fluctuates at ~ 1.25 eV (~ 1.26 to ~ 1.23 eV) for the $5\times 5\times 5$ k-mesh and at ~ 1.22 eV (~ 1.24 to ~ 1.22 eV) for the $6\times 6\times 6$ k-mesh. From the data lines shown in Fig. 5, we expect that the band gap will converge to ~ 1.2 eV when a much larger number of bands and k-points are employed in the G_0W_0 calculation.

Within the G_0W_0 approach, usually the quasiparticle wave function is very close to the LDA/GGA wave function, therefore the quasiparticle energy (E_{nk}^{QP}) can be calculated by

using only the diagonal matrix element of the self-energy operator [21]. As a result, the quasi-particle equation is reduced to [30]

$$E_{nk}^{QP} = \text{Re}[\langle \psi_{nk} | T + V_{ext} + V_H + \Sigma(E_{nk}^{QP}) | \psi_{nk} \rangle],$$

where the term $\Sigma(E_{nk}^{QP})$ is calculated using the LDA/GGA Kohn-Sham eigenvalues and eigenfunctions, and the eigenstates ψ_{nk} are approximated by the LDA/GGA wave functions. Thus, the convergence of the DFT-GGA wave functions will guarantee the convergence of the quasi-particle energy and consequently the value of band gap. Figure 6 shows the DFT-GGA total energy of β -PtO₂ as a function of k-mesh, for the calculations with a plane waves' energy cut-off of 400 eV and 600 eV, respectively. In both cases, the total energy is well converged (≤ 2 meV) when the employed k-mesh is equal to or denser than $6 \times 6 \times 6$. Within the framework of density functional theory (DFT), the total energy of a system is solely determined by the electron density. The convergence of total energy indicates the convergence of electron density, or alternatively the wave function of the system (differs by a phase factor at most). This result in return suggests that the calculated G_0W_0 band gap by using a $6 \times 6 \times 6$ k-mesh is close to convergence.

From the experimental side, the measured band gap of amorphous PtO₂ is ~ 1.2 eV [38], and that of α -PtO₂ ranges from ~ 1.3 eV [16] to 1.8 eV [17]. No experimental data is available for the band gap of β -PtO₂ yet. The reported resistivity for α -PtO₂ is on the order of $10^4 \Omega \cdot \text{cm}$ [39, 40] and that for β -PtO₂ is $\sim 10^6 \Omega \cdot \text{cm}$ [15]. Although the value of band gap is not the only factor that determines the resistivity of a material, it would be acceptable that the alpha and beta form of PtO₂ have similar band gap when considering their electrical resistivity.

In conclusion, we have studied the band gap of β -PtO₂ by DFT calculations. DFT-GGA calculation gives a band gap of ~ 0.46 eV, which is usually underestimated. The band gap is increased when the effective on-site Coulomb repulsion (U_{eff}) between the Pt 5d electrons is taken into account via the GGA+U method. In the case $U_{\text{eff}} \sim 7.5$ eV, which yields the best fit to the experimental lattice parameters, the calculated band gap is ~ 1.2 eV. The band gap given by conventional G_0W_0 approach is $\sim 1.25 \pm 0.05$ eV, which shows a tendency of converging to ~ 1.2 eV when the number of energy bands, the k-meshes and the energy cut-off for plane waves employed in calculation are increased to large values. The partially self-consistent GW_0 gives a band gap of ~ 1.28 eV and the self-consistent GW band gap is ~ 1.46 eV, which is expected to converge to a lower value (likely ~ 1.30 eV) when more accurate calculations are performed. The band gap given by HSE03 and HSE06 hybrid functional calculation is ~ 1.60 eV and 1.81 eV, respectively. The GW and HSE calculations indicate that the value of U parameter used in our recent work on oxygen-deficient β -PtO₂ [18] belongs to the range $U \geq 7.5$ eV. We hope that the predicted band gap can be tested by optical measurement in the future.

Acknowledgments

This work is supported by the Global Research Center for Environment and Energy based on Nanomaterials Science (GREEN) at National Institute for Materials Science (NIMS). The first-principles calculations were carried out by the supercomputer (SGI Altix) of NIMS.

References

- [1] M. D. Ackermann, T. M. Pedersen, B. L. Hendriksen, *et al.*, *Phys. Rev. Lett.* **95**, 255505 (2005).
- [2] X.-Q. Gong, R. Raval, and P. Hu, *Phys. Rev. Lett.* **93**, 106104 (2004).
- [3] W. X. Li and B. Hammer, *Chem. Phys. Lett.* **409**, 1 (2005).
- [4] X.-Q. Gong, Z.-P. Liu, R. Raval, and P. Hu, *J. Am. Chem. Soc.* **126**, 8 (2004).
- [5] H.-F. Wang, Y.-L. Guo, G. Lu, and P. Hu, *J. Phys. Chem. C* **113**, 18746 (2009).
- [6] B. E. Conway, *Prog. Surf. Sci.* **49**, 331 (1995).
- [7] H. Imai *et al.*, *J. Am. Chem. Soc.* **131**, 6293 (2009).
- [8] Y. Liu *et al.*, *Electrochemical and Solid-State Letters* **13**, B1-B3 (2010).
- [9] V. Voorhees, R. Adams, *J. Am. Chem. Soc.* **44**, 1397 (1922).
- [10] L. B. Hunt, *Platinum Metals Rev.* **6**, 150 (1962).
- [11] B. E. Conway *et al.*, *J. Chern. Phys.* **93**, 8361 (1990).
- [12] O. Muller and R. Roy, *J. Less-Common Metals* **16**, 129 (1968).
- [13] K.-J. Range, F. Rau, U. Klement, and A. M. Heyns, *Mat. Res. Bull.* **22**, 1541 (1987).
- [14] R. Wu and W. H. Weber, *J. Phys.: Condens. Matter* **12**, 6725 (2000).
- [15] R. D. Shannon, *Solid State Commun.* **7**, 257 (1969).

[16] C. R. Aita. *J. Appl. Phys.* **58**, 3169 (1985).

[17] Z. Jin *et al.*, *J. Mol. Catal. A: Chem.* **191**, 61 (2003).

[18] Y. Yang, O. Sugino and T. Ohno, *Phys. Rev. B* **85**, 035204 (2012).

[19] J. P. Perdew, K. Burke, M. Ernzerhof, *Phys. Rev. Lett.* **77**, 3865 (1996).

[20] L. Hedin, *Phys. Rev.* **139**, A796 (1965).

[21] M. S. Hybertsen and S. G. Louie, *Phys. Rev. B* **34**, 5390 (1986).

[22] J. Heyd, G. E. Scuseria, and M. Ernzerhof, *J. Chem. Phys.* **118**, 8207 (2003).

[23] J. Heyd and G. E. Scuseria, *J. Chem. Phys.* **121**, 1187 (2004).

[24] J. Heyd, G. E. Scuseria, and M. Ernzerhof, *J. Chem. Phys.* **124**, 219906 (2006).

[25] G. Kresse and J. Hafner, *Phys. Rev. B* **47**, 558 (1993).

[26] G. Kresse and J. Furthmüller, *Phys. Rev. B* **54**, 11169 (1996).

[27] P. E. Blöchl, *Phys. Rev. B* **50**, 17953 (1994).

[28] G. Kresse and D. Joubert, *Phys. Rev. B* **59**, 1758 (1999).

[29] S. L. Dudarev, G. A. Botton, S. Y. Savrasov, C. J. Humphreys, A. P. Sutton, *Phys. Rev. B* **57**, 1505 (1998).

[30] M. Shishkin and G. Kresse, *Phys. Rev. B* **74**, 035101 (2006).

[31] M. Shishkin and G. Kresse, *Phys. Rev. B* **75**, 235102 (2007).

[32] H. J. Monkhorst and J. D. Pack, *Phys. Rev. B* **13**, 5188 (1976).

[33] P. E. Blöchl, O. Jepsen and O. K. Andersen, *Phys. Rev. B* **49**, 16223 (1994).

[34] T. Miyake, P. Zhang, M. L. Cohen and S. G. Louie, *Phys. Rev. B* **74**, 245213 (2006).

[35] B.-C. Shih, Y. Xue, P. Zhang, M. L. Cohen and S. G. Louie, *Phys. Rev. Lett.* **105**, 146401 (2010).

[36] J. Paier, M. Marsman, K. Hummer, G. Kresse, I. C. Gerber, and J. G. Ángyán, *J. Chem. Phys.* **124**, 154709 (2006).

[37] C. Friedrich, M. C. Müller, and S. Blügel, *Phys. Rev. B* **83**, 081101(R) (2011).

[38] H. Neff *et al.*, *J. Appl. Phys.* **79**, 7672 (1996).

[39] D. Cahen, J. A. Ibers, and J. B. Wagner, Jr., *Inorg. Chem.* **13**, 1377 (1974).

[40] L. Maya, E. W. Hagaman, R. K. Williams, *et al.*, *J. Phys. Chem. B* **102**, 1951 (1998).

Figures and Captions

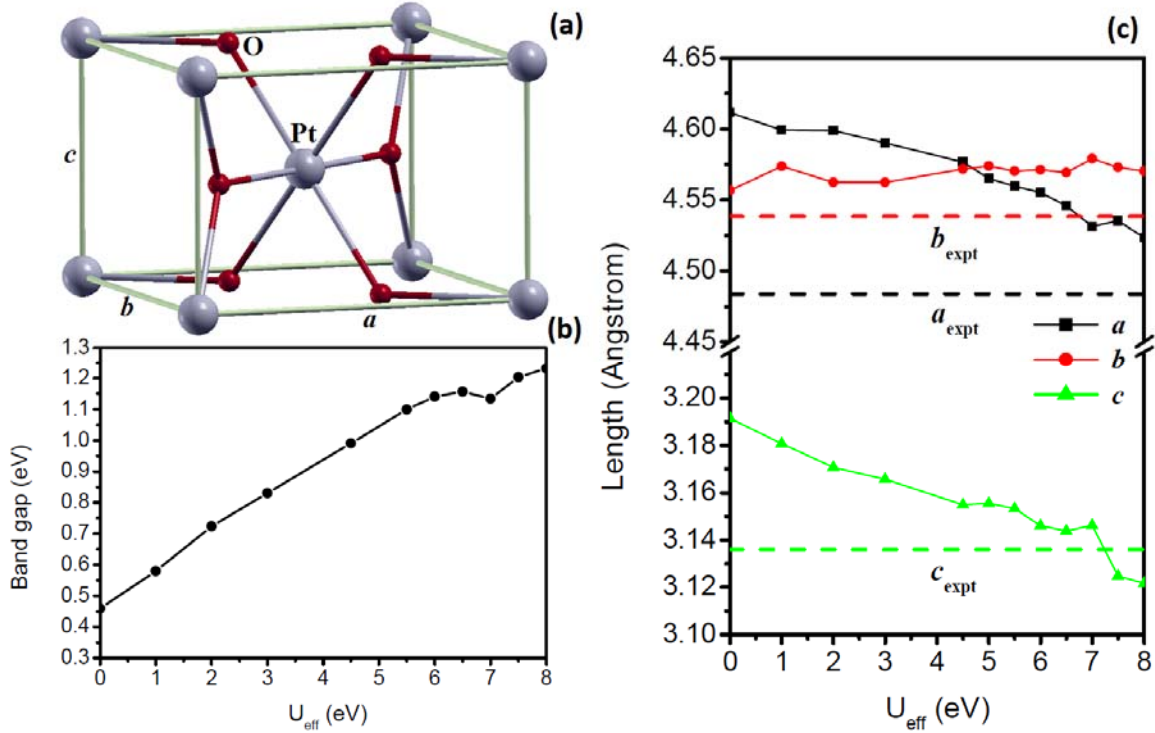


FIG. 1 (Color online) (a) Primitive cell of β -PtO₂. (b) Calculated band gap of β -PtO₂ as a function of effective on-site Coulomb repulsion (U_{eff}) in GGA+U method. (c) Optimized length of cell edges a , b , and c as a function of U_{eff} . The experimental values of a , b , and c (from Ref. [13]) are indicated by dashed lines.

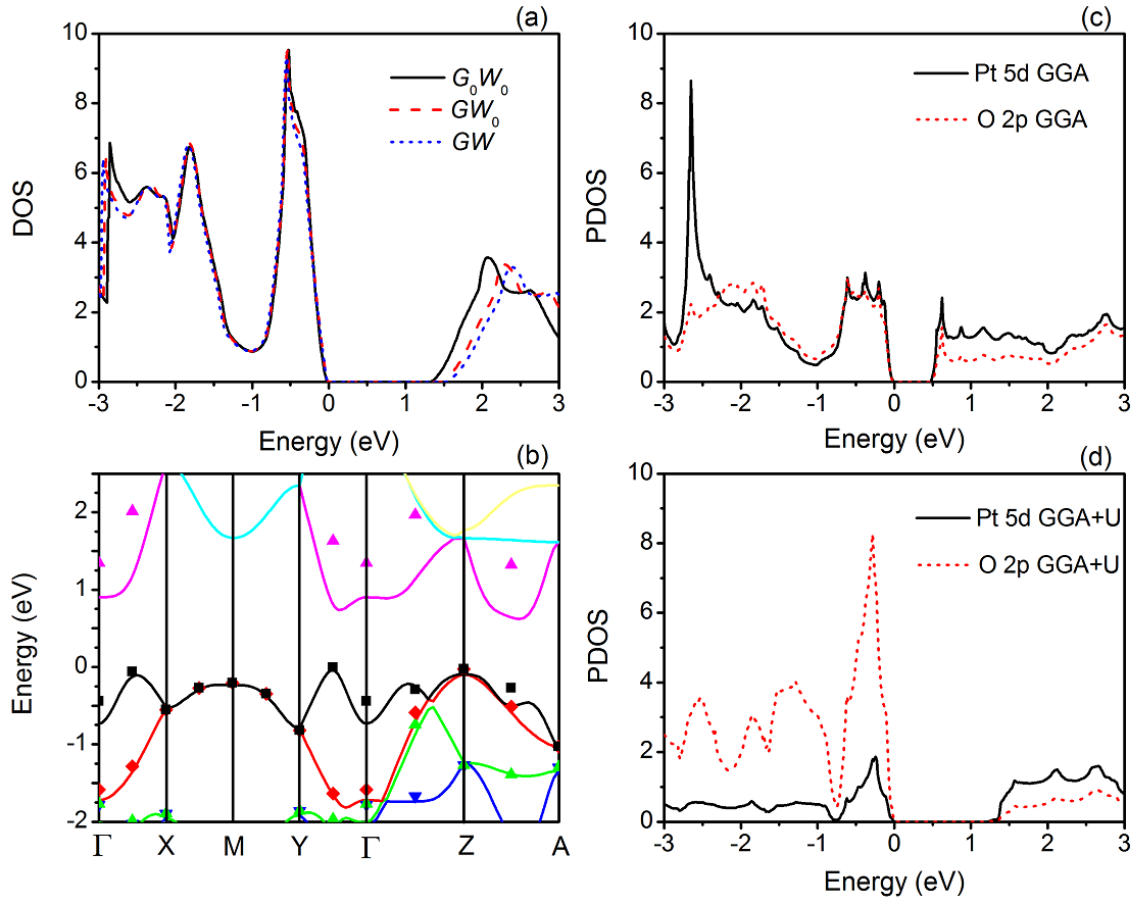


FIG. 2 (Color online) (a) Calculated electronic density of states (DOS) of β -PtO₂ by using one-shot G_0W_0 , partially self-consistent GW_0 and self-consistent GW method. (b) Energy bands of β -PtO₂, calculated using GGA (solid lines) and G_0W_0 method (scattered squares and triangles) along some lines joining the high-symmetry points in the k-space. The direct coordinates of the k-points in Brillouin zone (BZ): $\Gamma = (0, 0, 0)$, $X = (0.5, 0, 0)$, $M = (0.5, 0.5, 0)$, $Y = (0, 0.5, 0)$, $Z = (0, 0, 0.5)$, $A = (0.5, 0.5, 0.5)$. (c) The partial DOS (PDOS) of Pt 5d and O 2p orbitals from GGA calculations. (d) The PDOS of Pt 5d and O 2p orbitals from GGA+U calculations. For all the figures here and below, the highest occupied energy level is set at zero and the unit of DOS and PDOS is state/eV/cell.

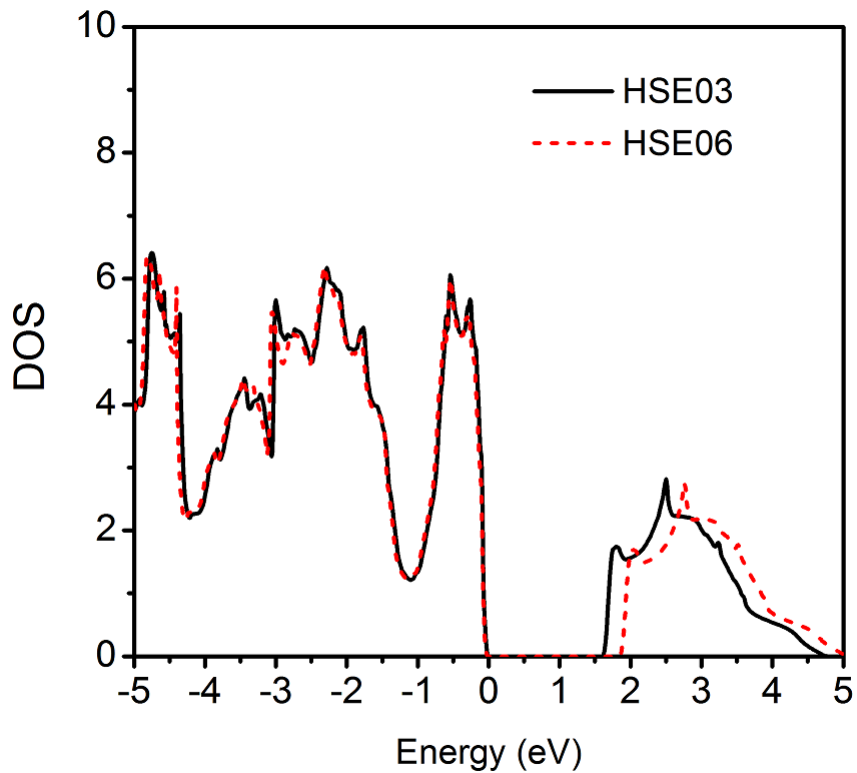


FIG. 3 (Color online) The electronic DOS of β -PtO₂, obtained from HSE03 and HSE06 hybrid functional calculations.

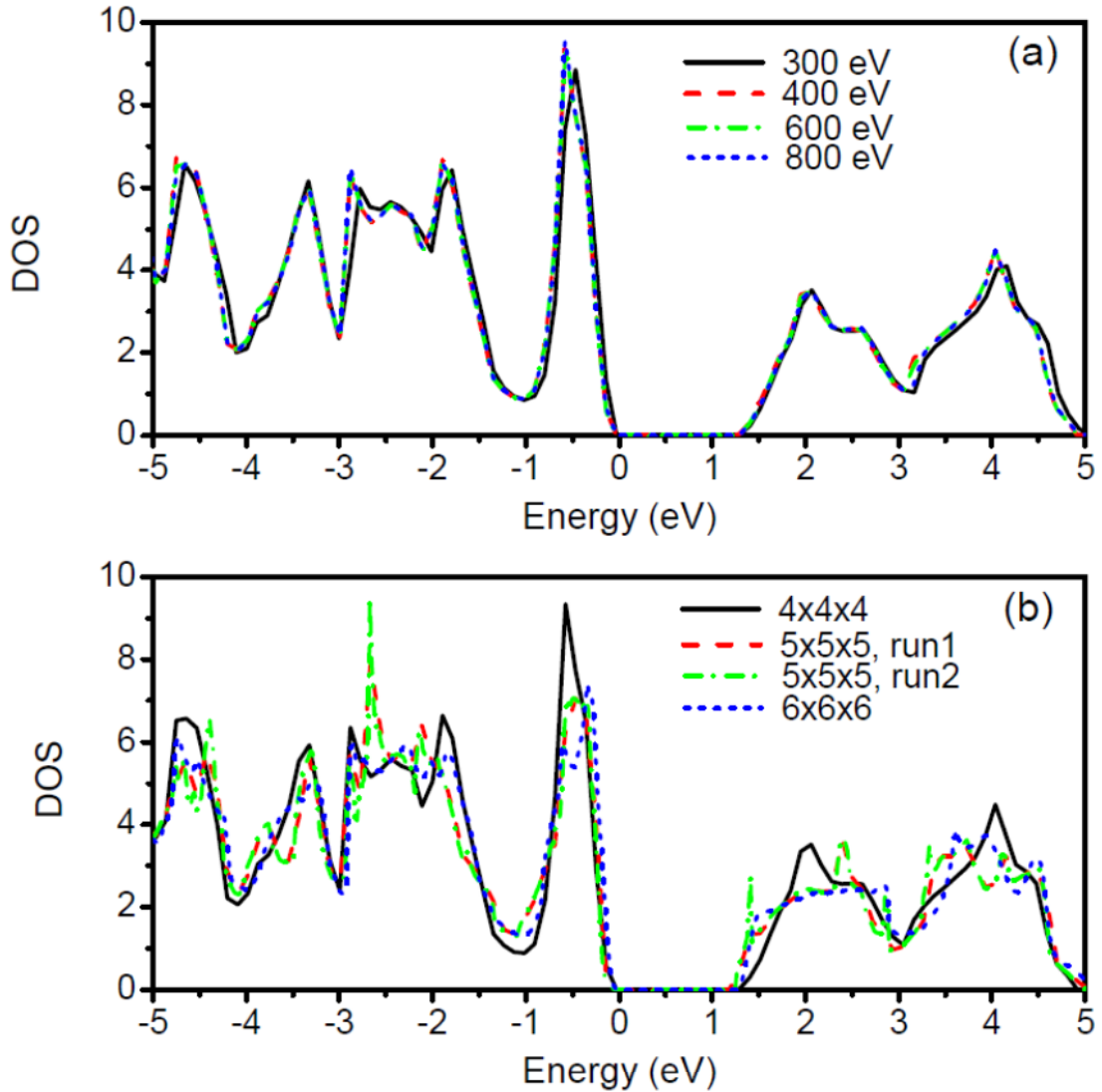


FIG. 4 (Color online) The G_0W_0 electronic DOS of β -PtO₂. (a) Results obtained from four calculations with different energy cut-off for plane waves. A $4 \times 4 \times 4$ k-mesh and 400 energy bands are used for each calculation. (b) Results from the calculations using four different k-meshes. The energy cut-off (ENCUT) and number of energy bands (NBAND) for both k-meshes $4 \times 4 \times 4$ and $5 \times 5 \times 5$ run1 are 600 eV and 400. The ENCUT and NBAND for both k-meshes $5 \times 5 \times 5$ run2 and $6 \times 6 \times 6$ are 400 eV and 450.

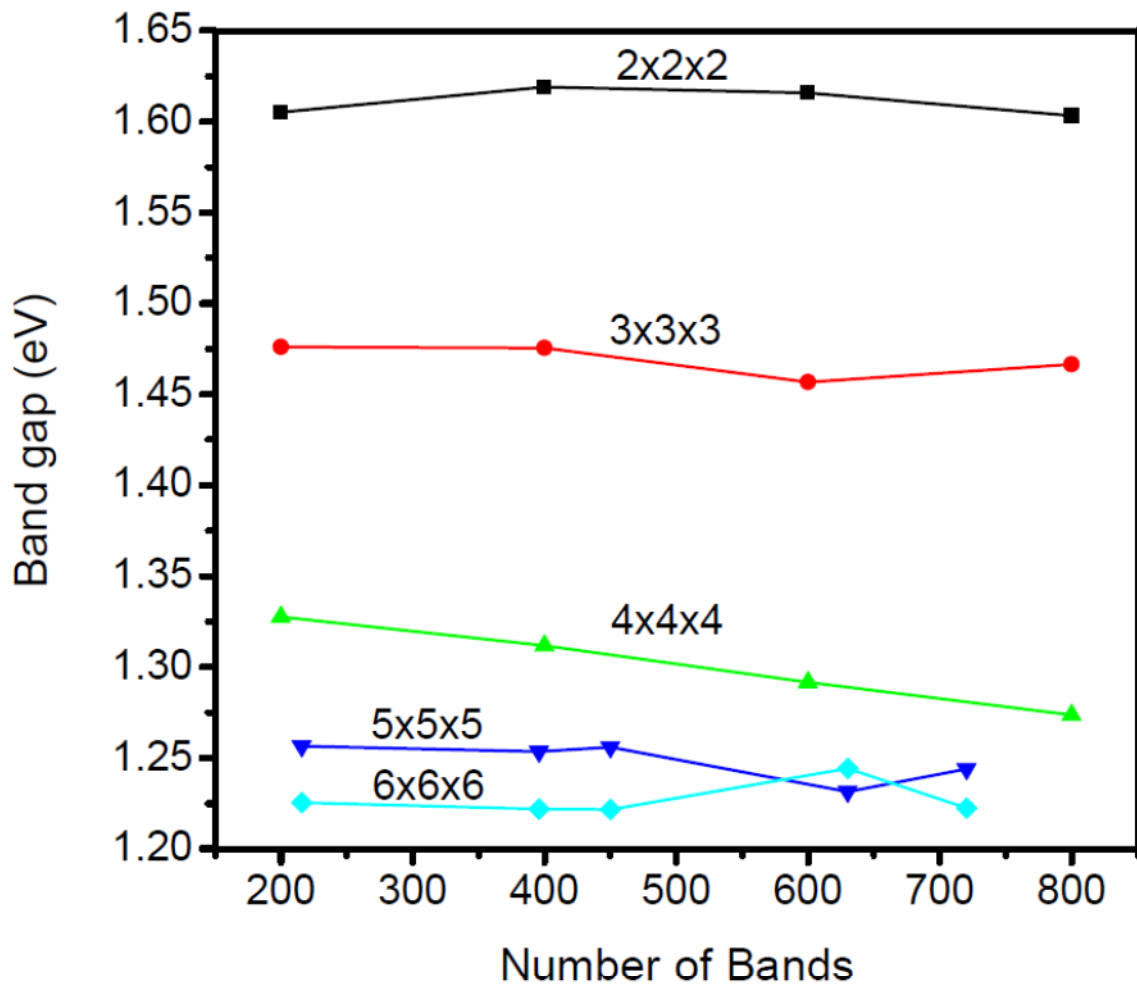


FIG. 5 (Color online) The G_0W_0 band gap of β -PtO₂, as a function of the number of energy bands and k-meshes involved in calculation. The plane waves' energy cut-off is 600 eV for k-meshes $2 \times 2 \times 2$, $3 \times 3 \times 3$, $4 \times 4 \times 4$ and $5 \times 5 \times 5$, and is 400 eV for the k-mesh $6 \times 6 \times 6$.

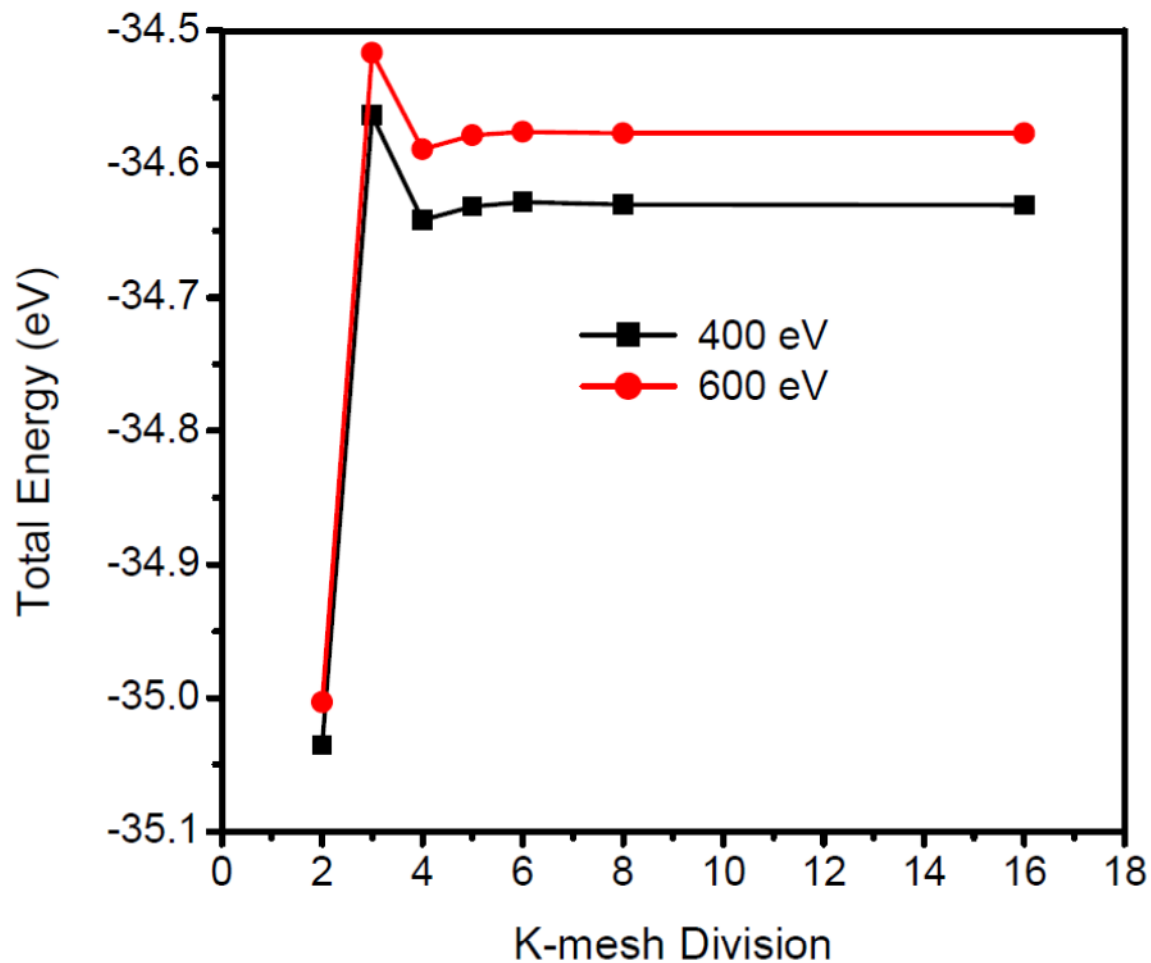


FIG. 6 (Color online) The DFT-GGA total energy of β -PtO₂, as a function of k-meshes employed in two calculations with a plane waves' energy cut-off of 400 eV and 600 eV. Each integer n on the k-mesh division axis corresponds to a uniform k-mesh of $n \times n \times n$.